Supplemental Figure 1

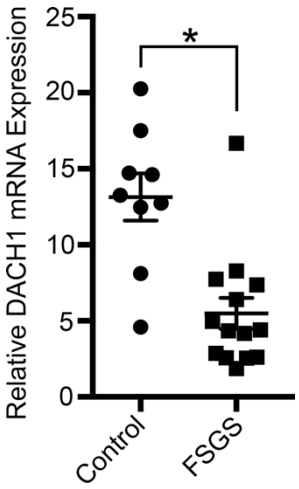

Supplemental figure 1. DACH1 expression is decreased in human FSGS. DACH1 mRNA expression is decreased in glomeruli from human FSGS kidney biopsy specimens (raw data available from Nephroseq). *P<.0003.

Supplemental figure 2

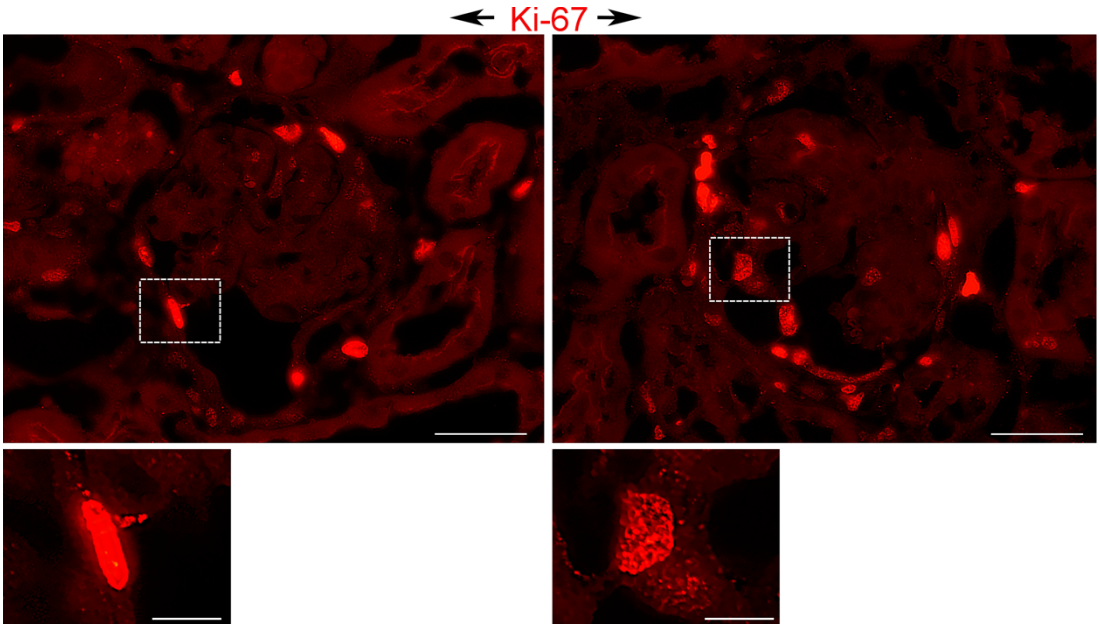

Supplemental figure 2. Immunofluorescence for Ki67 in podocyte-specific DACH1 KO mice exposed to STZ-induced hyperglycemia demonstrates robust parietal cell activation. Left inset shows Ki67 positive parietal cell beginning to extend towards areas of severe podocyte loss. Right inset shows typical vacuolated appearance of an activated parietal cell inside the glomerular tuft. Scale bars: lower power, 40μm; higher power inset, 10μm.

Supplemental Figure 3

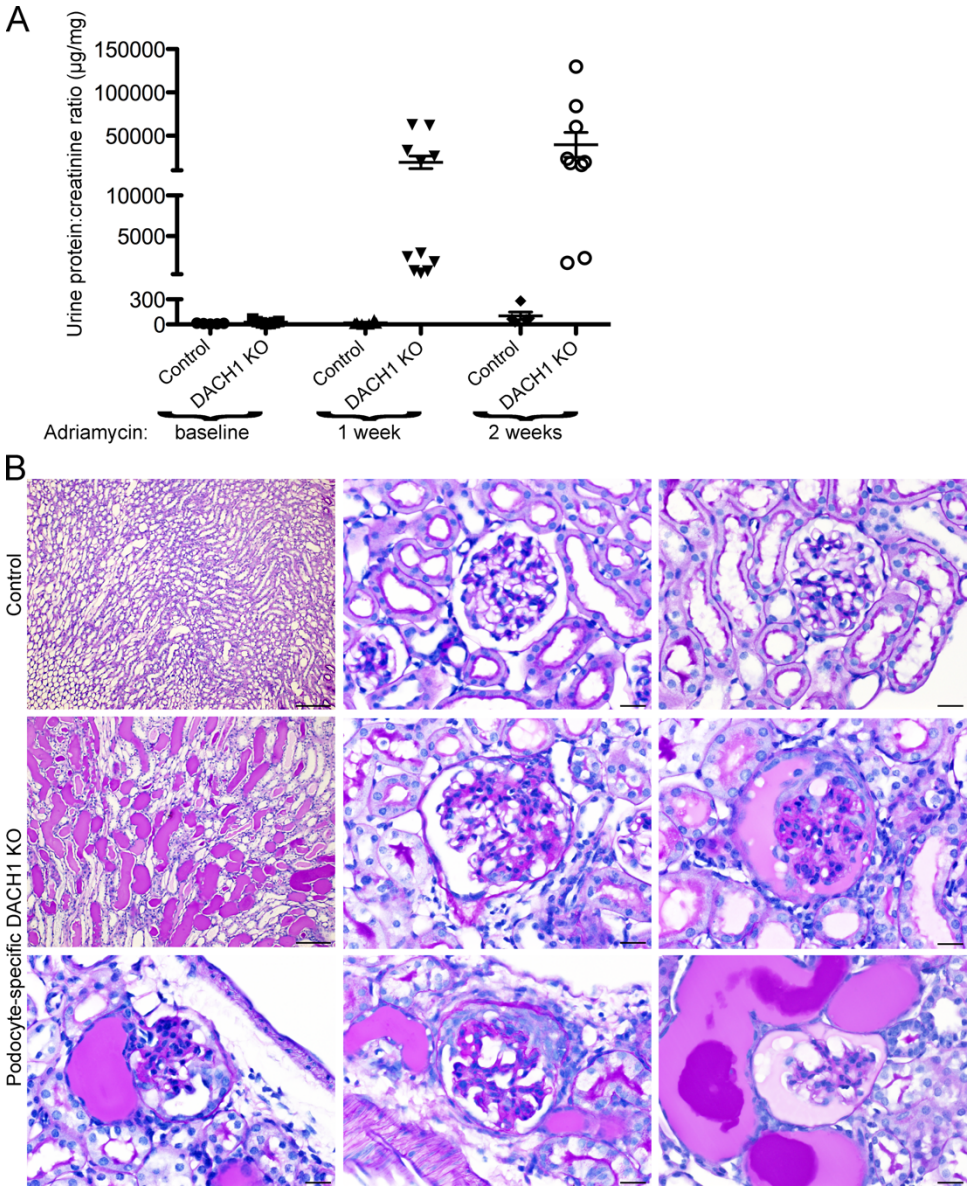

Supplemental figure 3. Podocyte-specific DACH1 KO mice are exquisitely sensitive to ADR-induced FSGS (A) Calculated urine protein:creatinine ratios demonstrate massive proteinuria in podocyte-specific DACH1 KO mice within 2 weeks after ADR administration compared to control littermates. **(B)** Histology in ADR treated podocyte-specific DACH1 KO mice include diffuse tubular proteinaceous casts with microcysts, mesangial expansion, diffuse and severe FSGS, some glomeruli show collapse with epithelial proliferation. ADR treated control mice demonstrated normal kidney histology. Scale bars: low power, 100µm; high power, 20µm.

Supplemental Figure 4

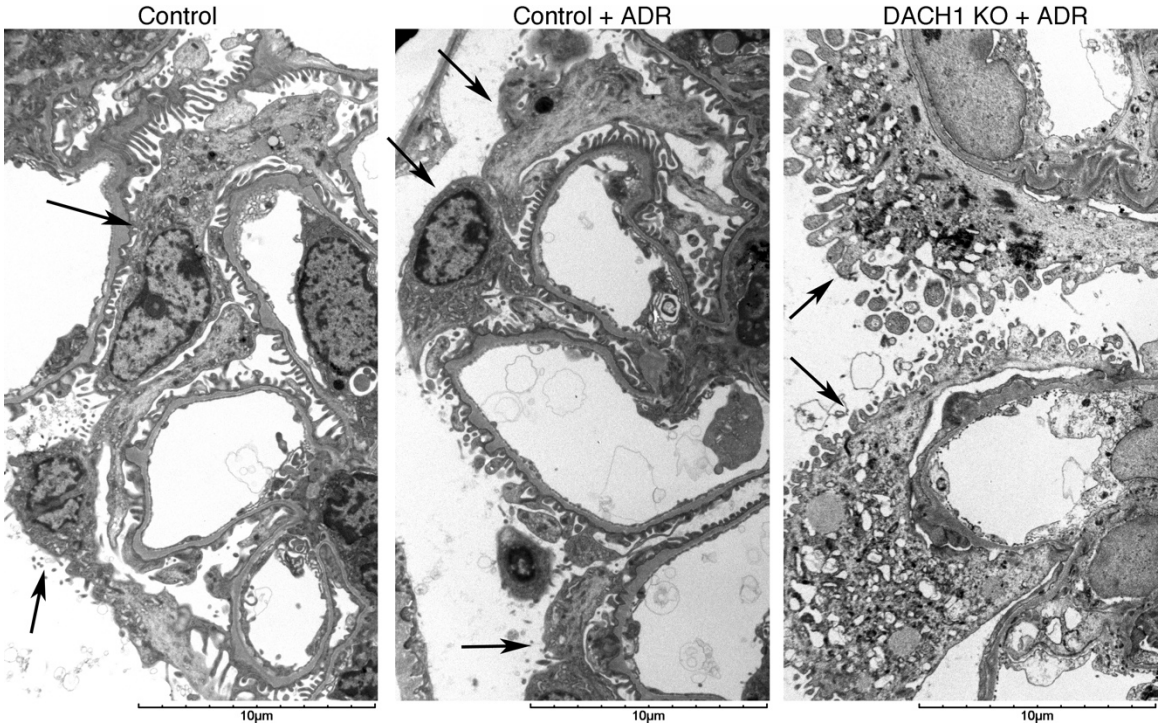

Supplemental figure 4. DACH1 KO podocytes show catastrophic injured after ADR on electron microscopy. Podocyte-specific DACH1 KO mice have normal podocyte morphology and intricate foot processes under the basal condition (left). Control mice are resistant to ADR nephropathy, showing only patchy areas of effacement (center). Podocyte-specific DACH1 KO mice are profoundly sensitive to ADR-induced injury with podocytes showing catastrophic damage including severe microvillous changes, cytoplasmic vacuolization, cellular hypertrophy, and complete loss of primary and secondary processes (right). Arrow, podocyte cell body.

Supplemental Figure 5

Upregulated:

Symbol	Description	Fold Change (baseline)	Fold change (early STZ)	*p*-value	DBD	PTIP KO mice
Prm1	protamine-1	+562	+2325	3.20E-08, 5.48E-08	yes	+
Pamr1	peptidase domain containing associated with muscle regeneration 1	+3.40	+7.40	.0009, 1.60E-06	yes	-
Itga2	integrin alpha 2	+1.99	+5.11	.0006, .0032	yes	-
Lrrc4	leucine rich repeat containing 4	+3.95	+4.96	.0005, .0009	yes	-
Mycl	v-myc avian myelocytomatosis viral oncogene lung carcinoma derived	+3.95	+2.78	.0003, .0001	yes	-
Astn2	astrotactin 2	+1.50	+2.53	.0427, 2.19E-05	yes	-
Adm	adrenomedullin	+1.99	+2.33	.0086, .0165	yes	+
Lrtm2	leucine-rich repeats and transmembrane domains 2	ND	+5.52	.0082	yes	+
Smyd1	SET and MYND domain containing 1	ND	+3.50	.0029	yes	-
Nell2	NEL-like 2	ND	+2.77	.0019	yes	-
Necab3	N-terminal EF-hand calcium binding protein 3	ND	+2.02	.0071	yes	-
Tspan32	tetraspanin 32	ND	+1.86	.0022	no	+
2410004 P03Rik	RIKEN cDNA 2410004P03 gene	ND	+1.76	.0021	no	+
Aff3	AF4/FMR2 family, member 3	ND	+1.75	.0005	yes	-
Ntrk3	neurotrophic tyrosine kinase, receptor, type 3	ND	+1.68	.0056	yes	-

Downregulated:

Symbol	Description	Fold Change (baseline)	Fold change (early STZ)	*p*-value	DBD	PTIP KO mice
Ptchd4	patched domain containing 4	-5.14	-2.87	.0136, .0001	no	-
Il6ra	interleukin 6 receptor, alpha	-1.90	-2.80	.0089, .0248	no	-
Ephb1	Eph receptor B1	-3.28	-1.95	.0363, .0003	no	-
Lingo2	leucine rich repeat and Ig domain containing 2	ND	-6.64	.0292	no	-
Padi4	peptidyl arginine deiminase, type IV	ND	-1.48	.0475	yes	+

Supplemental figure 5. Overlap of glomerular transcriptomes between podocyte-specific DACH1 KO mice and podocyte-specific PTIP KO mice. RNA sequencing was performed comparing podocyte-specific DACH1 KO mice (both at baseline and early after STZ induced hyperglycemia) to control littermates, and differentially expressed genes were compared to a previously reported microarray of podocyte-specific PTIP KO mice (38). Overlapping genes are shown. Fold changes and *p*-values are displayed for podocyte-specific DACH1 KO mice. ND, no difference. Presence or absence of a promoter DACH1 binding domain (DBD) is also shown. Direction of regulation of each gene in PTIP KO mice is exhibited in last column.

Supplemental Figure 6

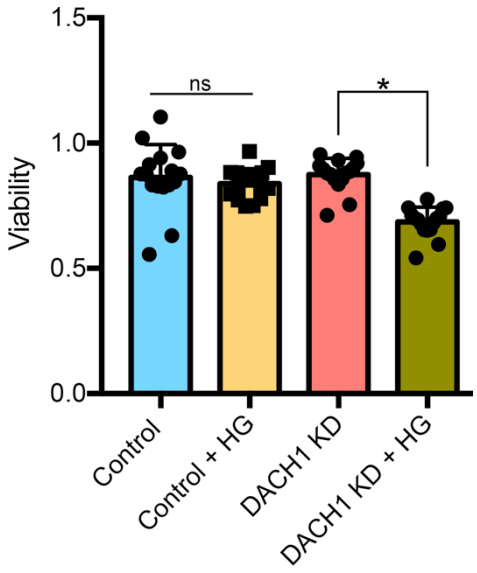

Supplemental figure 6. DACH1 knockdown podocytes show reduced viability when exposed to hyperglycemia. Viability of control podocytes was not altered by hyperglycemia and was similar to DACH1 knockdown podocytes grown in normal glucose. *P<.0001

Supplemental Figure 7

qPCR:
NELL2: GCACAAGCTCTCCTTAGCCAT and AGGGCTTTTCTACTACCCTTTCA
NTRK3: CTTTGCCCAGCCAAGTGTAGT and CGTGATGTTGATACTGGCGTT
PAMR1: GCAGTTGGGGCTCACTTTTC and CCCACGACTTCCCTCTTTCC
MYCL1: CTGCGGGGAGGATTTCTACC and CATGCAGTCACGGCGTATGAT

ChIP qPCR:
SV40: F1-TGCATCTCAATTAGTCAGCAACC, R1-GAATAGCTCAGAGGCCGAGG
Luc+: F2-ATCCGCTGGAAGATGGAACC, R2-TGCCAACCGAACGGACATTT

NELL2: P1: GGGTCTCCACGCTTTATTTG and AGAGAACTTGGCCAGGAGGT
P2: GTACCCACATGTTTGCATGG and GCATTCCACTTTCATTTTGGA
NTRK3: P1: AGCGTCTGGCTGGACTATGT and CCGGCAATTGATCTCAGTCT
P2: AGGAAGACGCTCCGATAACC and CGGCTGCAGAAATGTACAAG

Supplemental figure 7. qPCR and ChIP qPCR primer sequences.